communications medicine

A Nature Portfolio journal

Article

Article in Press

https://doi.org/10.1038/s43856-026-01978-9

A revised visual grading scale of the cavum septi pellucidi in contact-collision sport athletes with repetitive head impacts

Check for updates

Anya S. Mirmajlesi[1,2,40], Jared Stearns[1,2,40], Brian Szekely[1,2,40], Manuel Estrada[1,2], Rebecca D. Folkerth[3], Sylvain Bouix[4], Daniel H. Daneshvar[5,6,7], Charles H. Adler[8], Charles Bernick[9,10], Laura J. Balcer[11,12,13], Jeffrey L. Cummings[14], Eric M. Reiman[15,16,17,18], Robert A. Stern[19,20,21], Martha E. Shenton[22,23,24], Richard J. Rushmore[20,22,40], Hector Arciniega[1,2,25,40] ✉ & for the DIAGNOSE CTE Research Project*

Abstract

Background The cavum septi pellucidi (CSP), a persistent separation between the septal leaflets in the brain, is found among athletes exposed to repetitive head impacts (RHI), yet existing grading systems may inadequately capture anatomical variants. This study presents a revised CSP grading scale for RHI-exposed populations.

Methods This cross-sectional study included 170 former American football players and 54 unexposed asymptomatic controls, all males aged 45-74, who underwent magnetic resonance imaging. Two blinded raters independently applied a revised 5-point CSP grading scale, with reliability assessed using Cohen's κ. CSP length and volume were quantified, and associations with cumulative head impact exposure were examined. Multivariable ordinal logistic regression compared CSP grades between former football players and controls.

Results Following consensus ratings, former football players demonstrated significantly greater odds of being classified into a higher CSP grade than unexposed controls (OR = 4.41, [95% CI: 2.34, 8.31], $p < 0.001$). CSP length and volume increased across CSP grade (both $p < 0.001$), supporting the anatomical validity of the revised grading system. Among former football players, estimated cumulative linear and rotational head impact exposures differed significantly across CSP grades (Kruskal–Wallis $p = 0.007$ and $p < 0.001$, respectively), with Grade 4 showing greater exposure than Grade 0.

Conclusion A revised CSP grading scale incorporating posterior variants shows high inter-rater reliability and concordance with quantitative measures in RHI-exposed athletes. More severe CSP morphology was associated with greater cumulative biomechanical exposure, and the revised grading system enables consistent classification of CSP morphology for future RHI studies.

Plain language summary

A small fluid-filled space in the brain called the cavum septi pellucidi (CSP) is often seen on MRI scans of athletes with histories of repeated head impacts (RHI). However, existing visual grading systems may miss forms of CSP, especially when it extends toward the back of the brain. We developed a revised 5-point MRI grading scale and tested it in 170 former American football players and 54 unexposed controls without a history of RHI. The new scale matched precise CSP size measurements and showed strong rater agreement. More severe CSP grades were associated with lifetime head-impact exposure, suggesting that RHI may contribute to these brain changes and serve as a better tool for long-term brain health research.

Repetitive head impacts (RHI) sustained over years of participation in contact and collision sports have increasingly been linked to structural brain alterations detectable during life[1–7]. As efforts to characterize the in vivo consequences of RHI have expanded, attention has focused on brain structures that may be particularly vulnerable to repeated mechanical stress. One such structure is the cavum septi pellucidi (CSP), a persistent separation of the septal leaflets between the lateral ventricles formed by the corpus callosum and fornix[8–11]. The CSP has emerged as a consistently reported neuroimaging finding in contact- and collision-sport athletes and may be a potential imaging marker of RHI, with studies demonstrating higher prevalence and increased length compared with control populations[7,12–19]. These observations have motivated the use of grading scales to characterize CSP morphology and to relate structural variation to neuropsychiatric[20–23] and neurodegenerative outcomes associated with RHI[7,12,13,16,24].

A full list of affiliations appears at the end of the paper. ✉e-mail: hector.arciniega@nyulangone.org

Table 1 | Demographics

Characteristics	Former Football Players(n = 170)	Controls (n = 54)
Age, median (IQR)	56 (51-64)	59.5 (52.3-67)
BMI, median (IQR) kg/m^2	32.2 (28.9-36.0)	30.4 (27.8-33.1)
Years of education, median (IQR), y	16 (16-18)	16 (16-18)
APOE ε4 carrier, n(%)	48 (29.3)	10 (19.6)
Race, n (%)		
White	108 (63.5)	34 (63)
Black/African American	59 (34.7)	19 (35.2)
American Indian/Alaska Native	0 (0)	0 (0)
Asian	0 (0)	0 (0)
Native Hawaiian/Other Pacific Islander	0 (0)	1 (1.8)
Multiple Races	3 (1.8)	0 (0)
Exposure to RHI		
Age of first exposure to football, mean (SD), y	11.1 (2.8)	
Total years of football played, mean (SD), y	15.9 (4.3)	
CHII-Frequency, median (IQR) impacts x 10^3	9.6 (7.7–13.1)	
CHII-Linear Acceleration, median (IQR) g-force x 10^5	2.2 (1.8–2.7)	
CHII-Rotational Acceleration, median (IQR) radians/s^2 x 10^7	1.8 (1.4–2.2)	
Position Played, n (%)		
Offensive Linemen	41 (24)	
Offensive Backs and Receivers	48 (28)	
Defensive Linemen	18 (11)	
Linebackers	26 (15)	
Defensive Backs	33 (19)	
Special Teams	4 (3)	

Overview of cohort characteristics, including demographics of 170 former football players and 54 unexposed asymptomatic controls. APOE ε4-carrier analysis was only available for 164 former players and 51 controls. Abbreviations: *BMI* Body Mass Index, *RHI* Repetitive Head Impacts, *CHII* Cumulative Head Impact Index, *y* years, *IQR* Interquartile Range, *SD* Standard Deviation.

Early neuroimaging work introduced visual grading schemes to characterize CSP width in clinical populations[21,22]. These approaches were subsequently applied to cohorts exposed to RHI[12,16,18,24,25]. However, existing CSP grading systems were not developed for RHI-exposed populations and have limited capacity to capture the full spectrum of septal morphologies observed in contact and collision sport athletes[7,14,18,19]. These methods have largely relied on qualitative, width-based assessments, overlooking posterior extensions and complex variants such as *cavum vergae* and mixed or fenestrated configurations (CSP *et vergae*)[26–30]. These posterior and mixed morphologies are frequently observed in athletes with extensive RHI exposure, both during life and at postmortem examination, yet remain insufficiently represented in existing grading frameworks[1,7,31]. As a result, associations between CSP morphology and RHI exposure may be underestimated.

In the present study, we develop and evaluate a revised visual CSP grading scale designed to capture a broader range of septal morphology in individuals exposed to RHI, including posterior extension and septal leaflet discontinuity. We assess the reliability of the revised scale, examine its correspondence with quantitative measures of CSP length and volume, and investigate associations with cumulative RHI exposure. We find that the revised scale demonstrates high inter-rater reliability, with increasing CSP grades corresponding to greater CSP length and volume. Former American football players have greater odds of higher CSP grades than unexposed asymptomatic controls, and the most severe CSP morphology is associated with greater cumulative linear and rotational head impact exposure.

Methods

Study design and participants

This study was conducted as part of the multi-site Diagnostics, Imaging, and Genetics Network for the Objective Study and Evaluation of Chronic Traumatic Encephalopathy (DIAGNOSE CTE) Research Project[32]. Written informed consent was obtained from all participants before enrollment. Former college and professional American football players and unexposed asymptomatic controls were recruited for this cross-sectional study. Data were collected between September 2016 and February 2020. Of 180 enrolled former football players, 10 were excluded due to missing or poor-quality structural MRI, yielding an analytic sample of 170 participants. Of the 60 unexposed, asymptomatic controls initially included, six were excluded because of poor-quality structural MRI data, preexisting psychiatric conditions, or a history of RHI exposure, resulting in a final sample of 54 controls. Detailed recruitment procedures and eligibility criteria have been published previously and are provided in Supplementary Fig. 1 and Supplementary eTable 1. Demographic characteristics are presented in Table 1 and Supplementary eTable 2. The study was approved by the institutional review boards at all participating sites (Boston University Medical Campus IRB #H-34799, Mayo Clinic IRB #16-002662, Cleveland Clinic Lou Ruvo Center for Brain Health Banner IRB #16-1694, Alzheimer's Institute IRB #1168489, New York University Langone Health IRB# i16-01032 CR3, and Partners Healthcare/Brigham and Women's Hospital IRB #2016P001359 and #2016P001328). Reporting adheres to STROBE guidelines and ethical standards set by the Declaration of Helsinki.

MRI

Image acquisition. All participants underwent a head MRI scan at one of four neuroimaging sites: Brigham and Women's Hospital, NYU Langone Medical Center, the Cleveland Clinic Lou Ruvo Center for Brain Health (Las Vegas), or Mayo Clinic Arizona. The imaging protocol included structural MRI, diffusion MRI, functional MRI, and magnetic resonance spectroscopy sequences. The structural images were acquired on a 3 T scanner (Siemens Magnetom Skyra, Erlangen, Germany; software version VE11) using a 20-channel head coil. Of relevance to this study is the high-resolution 3D T1-weighted magnetization-prepared rapid gradient-echo (MPRAGE) sequence with a voxel size of 1 × 1 x 1 mm^3, an inversion time = 1100 ms, TR = 2530 ms, TE = 3.36 ms, a 7-degree flip angle, and a 256 FOV. Raw T1-weighted structural images were processed using the FreeSurfer v7.4.1 *recon-all* pipeline, which included correction for inhomogeneity, signal intensity normalization, and skull stripping.

Visual CSP grading scale

To revise the CSP grading scale, two independent raters (A.S.M. and J.S.) were trained by an expert rater (H.A.) to identify the presence of the CSP and its variants (CSP *et vergae* and CSP *et cavum vergae*)[7]. Each rater independently examined all MRI scans from former American football players and unexposed controls. All MRI scans were de-identified and graded in a blinded fashion, such that raters were unaware of participant group assignment during CSP grading. The raters identified the presence of CSP (and variants, if applicable) and assigned a grade based on the revised grading scale, which incorporates CSP variants. This scale ranged from 0 to 4, where Grade 0 was defined as either an intact septum pellucidum without a visible CSP or a CSP visible on only a single coronal section. A CSP was required to extend across at least two contiguous coronal slices to be classified as Grade 1 or higher. Grade 1 is characterized by a separation of the septal leaflets that extends no more than a few millimeters in the anterior-posterior axis. Grade 2 is defined by a distinctly longer CSP, often extending

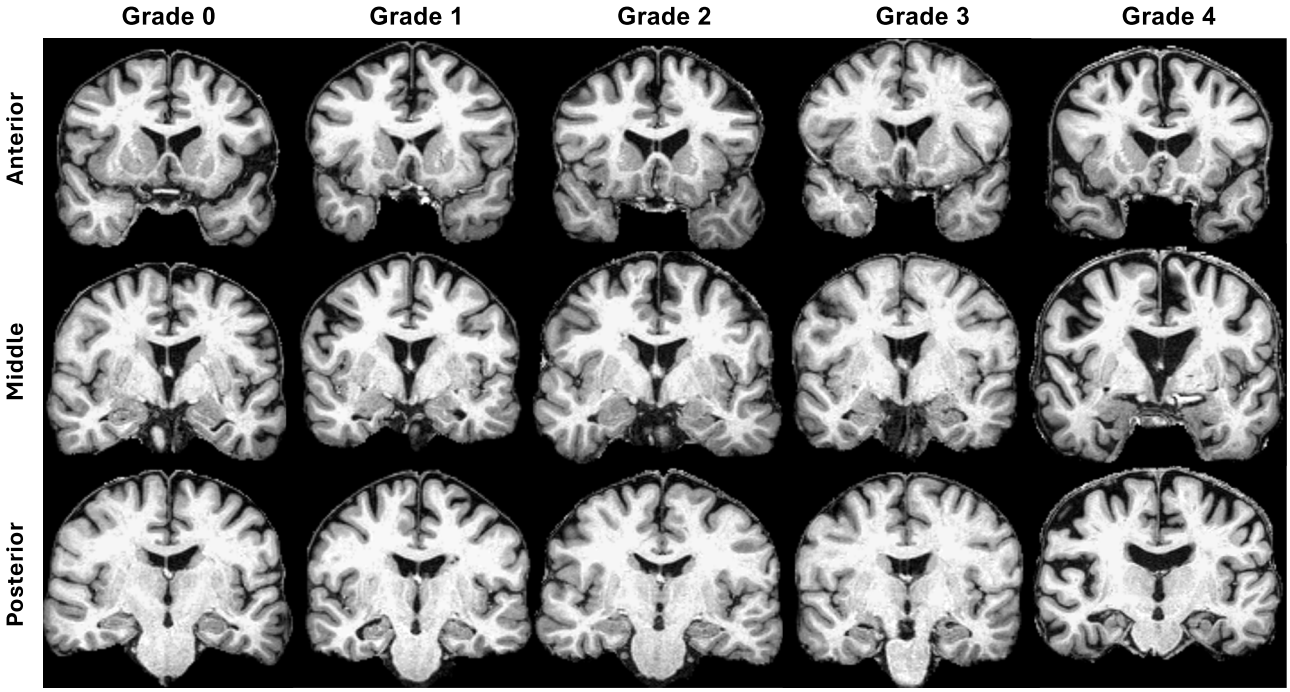

Fig. 1 | Coronal MRI slices of five separate participants depicting the revised CSP grading scale. Grade 0: Intact septum pellucidum without a visible CSP, or a CSP visible on only a single coronal slice. Grade 1: characterized by a space extending a few millimeters posterior to the genu. Grade 2: CSP extending posteriorly but remaining anterior to the columns of the fornix and the interventricular foramen of Monro. Grade 3: CSP extending posterior to the columns of the fornix and the foramina of Monro (CSP *et vergae*). Grade 4: CSP et cavum *vergae*, with marked septal leaflet disruption, in which one or both leaflets are no longer continuously visualized because of large discontinuities or apparent fenestrations. Slice images are shown at different coronal levels to illustrate the defining anatomical features of each grade.

posterior to the rostrum of the corpus callosum, but remaining anterior to the columns of the fornix and the interventricular foramen of Monro. Grade 3 is noted when the CSP extends posterior to the columns of the fornix and the foramen of Monro, also referred to as a CSP *et vergae*[10,26]. Grade 4 is defined as a CSP *et cavum vergae* in which one or both septal leaflets are no longer continuously visualized because of marked discontinuity or apparent fenestration, precluding reliable delineation of an intact septal boundary (see Fig. 1 and Supplementary eVideo 1). When features of multiple grades were present, cases were assigned to the highest applicable grade. Specifically, evidence of septal leaflet discontinuity or fenestration superseded posterior extension alone, and such cases were classified as Grade 4. Once all MRI scans were graded, the two raters deliberated to reach a final consensus on any disagreed-upon grades.

Objective CSP measurements

CSP volume. We applied a manual CSP segmentation protocol developed by our expert neuroanatomist (R.J.R.)[33]. Two independent raters (A.S.M. and M.E.), trained to criterion by R.J.R., manually segmented the CSP on T1-weighted images. Volumetric segmentation was performed only for Grades 1–3; Grade 0 participants were not segmented because CSP was absent or visible on only a single coronal section, whereas Grade 4 was excluded because septal leaflet discontinuity precluded reliable boundary delineation. Grade 0 participants were assigned a CSP volume of zero for statistical analyses. CSP volumes were then computed, normalized to the estimated total intracranial volume (eTIV) derived with *FreeSurfer v7.4.1*, and averaged across the two raters.

CSP length. CSP length was measured following our group's prior protocol[7]. CSP length was quantified for Grades 0–3; Grade 4 was excluded because septal leaflet discontinuity precluded reliable determination of CSP extent. Specifically, raters counted the number of contiguous coronal slices in which the CSP was visible and multiplied by the slice thickness (1 mm) to obtain length in millimeters. All CSP grading and volumetric segmentations were performed on T1-weighted images in 3D Slicer (v5.2.1)[34].

RHI exposure variables

Cumulative RHI exposure during American football participation was estimated using three previously derived metrics called the Cumulative Head Impact Index (CHII)[35]. CHII-frequency, representing total impact frequency; CHII-linear acceleration, representing cumulative linear acceleration (g-force); and CHII-rotational acceleration, representing cumulative rotational acceleration (radians/s^2). These indices integrate self-reported football history with position- and level-specific exposure estimates derived from helmet-based sensor data. Higher CHII values indicate greater lifetime RHI exposure. Full computational details have been published previously.

Statistics and reproducibility

Statistical analysis was performed using SPSS software version 29. First, inter-rater reliability for the visual CSP grading was evaluated using Cohen's κ coefficient. Next, to evaluate the precision of the manual segmentation protocol, we calculated the Dice similarity coefficient (Sorensen–Dice index) between segmentations from both raters. To normalize CSP volumes across all individuals, we divided individual CSP volumes by the respective intracranial volume. Differences in CSP-normalized volume, length, and CHII variables across grading scales were assessed using Kruskal–Wallis tests for global effects followed by Mann–Whitney U comparisons, given the non-parametric distribution of all variables. Multiple comparisons were controlled using the false discovery rate (FDR), with all FDR-adjusted p-values < 0.05 considered statistically significant.

To determine whether football players had greater odds of being classified into a higher CSP grade than unexposed asymptomatic controls, we fit a multivariable ordinal logistic regression model with CSP grade as the ordered outcome and the group as the primary predictor. The model was

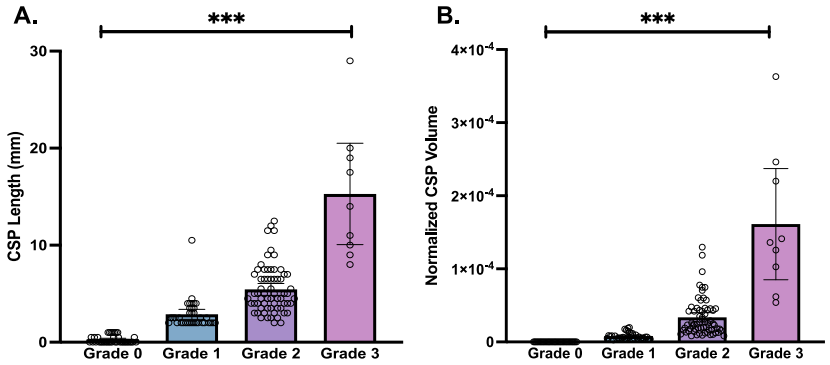

Fig. 2 | Quantitative validation of CSP grading. **A** CSP length (mm) ($n = 147$, $p = 1.67 \times 10^{-24}$) and **B** CSP volume normalized to the estimated total intracranial volume showing significant increases across higher CSP grades in former American football players ($n = 147$, $p = 2.21 \times 10^{-26}$), supporting the validity of the revised scale. *** $p < 0.001$. Error bars indicate 95% confidence intervals around the mean. Grade 4 was excluded because septal leaflet discontinuity precluded reliable measurement of CSP length and volume. A Kruskal-Wallis test followed by a Mann-Whitney U test was conducted for (**A**) and (**B**). All tests were two-sided, and adjustments were made for multiple comparisons. Abbreviation: CSP Cavum septi pellucidi.

adjusted for imaging site, APOE ε4 carrier status, age, eTIV, BMI, and years of education. Continuous covariates were standardized before model estimation. Model coefficients were exponentiated and reported as odds ratios (OR) with 95% confidence intervals. Statistical significance was defined a priori as $p < 0.05$.

Results

Demographic differences

The BMI was significantly higher in former American football players than in unexposed asymptomatic controls (mean difference = 1.77 kg/m^2, Welch's t = 2.35, [95% CI: 0.27, 3.26], p = 0.024). None of the remaining demographic variables differed significantly between groups (Table 1).

Revised CSP grading scale

Inter-rater reliability for the visual grading scale was excellent, with a Cohen's κ of 0.92 (p < 0.001). Following consensus ratings, CSP grades were distributed as follows for former American football players: Grade 0, 37/170 (21.8%); Grade 1, 36/170 (21.2%); Grade 2, 65/170 (38.2%); Grade 3, 9/170 (5.3%); and Grade 4, 23/170 (13.5%). Among unexposed asymptomatic controls, CSP grades were distributed as follows: Grade 0, 28/54 (51.9%); Grade 1, 12/54 (22.2%); Grade 2, 13/54 (24.1%); Grade 3, 0/54 (0%); Grade 4, 1/54 (1.9%); see Supplementary eTable 3. Representative coronal slices illustrating CSP severity across grades are shown in Fig. 1 and Supplementary eVideo 1. In the ordinal logistic regression model, former American football players had significantly greater odds of being classified into a higher CSP grade than unexposed asymptomatic controls (OR = 4.41, [95% CI: 2.34, 8.31], $p < 0.001$); see Supplementary eTable 3 for distribution of the unexposed asymptomatic controls.

CSP volume

Agreement between raters' volumetric segmentations was high, with an average Dice similarity coefficient of 0.847 [95% CI: 0.83, 0.87] among participants with CSP Grades 1–3. Because Grade 4 volume cannot be quantified, the final sample included 147 former American football players. Among these players, CSP volume increased significantly across CSP grades ($H(3) = 122.52$, $p < 0.001$). Grade 3 (mean, $1.61 \times 10{-}^{4}$ [95% CI: $8.51 \times 10{-}^{5}$, $2.37 \times 10{-}^{4}$]) participants also exhibited larger volumes compared to Grade 1 (mean, $7.98 \times 10{-}^{6}$ [95% CI: $6.42 \times 10{-}^{6}$, $9.55 \times 10{-}^{6}$]; U = 324, $p < 0.001$), and Grade 2 (mean, $3.36 \times 10{-}^{5}$ [95% CI: $2.72 \times 10{-}^{5}$, $4.00 \times 10{-}^{5}$]; U = 564, $p < 0.001$). Representative examples of normalized CSP volume across grades are shown in Fig. 2B and Table 2.

CSP length

Descriptive analyses showed a parallel pattern to CSP volume when evaluating CSP length. Following the exclusion of Grade 4 cases that could not be quantified, the final sample included 147 former American football players. Among the former football players, the CSP length also increased significantly across CSP grades ($H(3) = 113.81$, $p < 0.001$). Participants categorized in Grade 3 exhibited longer CSP structures (mean, 15.28 [95% CI: 10.05, 20.50]) compared to Grade 0 participants (mean, 0.27 mm [95% CI: 0.14, 0.40]; U = 333, $p < 0.001$). Grade 3 participants also exhibited greater CSP length than participants in Grade 1 (mean, 2.88 mm [95% CI: 2.36, 3.39]; U = 321, $p < 0.001$) and Grade 2 (mean, 5.45 mm [95% CI: 4.83, 6.06]; U = 564, $p < 0.001$). Representative examples of CSP length across grades are shown in Fig. 2A and Table 2.

CSP grade and cumulative head impact exposure

Among the 170 former American football players, CHII-frequency did not differ significantly across CSP grades ($H(4) = 1.92$, $p = 0.75$), with similar mean values by grade Grade 0: 1.08×10^4 [95% CI: 9.32×10^3, 1.22×10^4]; Grade 1: 1.10×10^4 [95% CI: 9.29×10^3, 1.27×10^4]; Grade 2: 1.03×10^4 [95% CI: 9.29×10^3, 1.14×10^4]; Grade 3: 1.12×10^4 [95% CI: 6.74×10^3, 1.58×10^4]; and Grade 4: 1.22×10^4 [95% CI: 9.79×10^3, 1.46×10^4]). In contrast, cumulative linear and rotational head impact exposure differed significantly across CSP grades, with the highest exposure observed among participants classified as Grade 4. For CHII-linear acceleration, the overall Kruskal-Wallis test was significant ($H(4) = 13.97$, $p = 0.007$). Participants with Grade 4 CSP had higher CHII-linear acceleration (mean, 2.83×10^5 [95% CI: 2.50×10^5, 3.16×10^5]) than those with Grade 0 (mean, 2.20×10^5 [95% CI: 1.97×10^5, 2.42×10^5]; U = 217, $p = 0.002$), Grade 1 (mean, 2.18×10^5 [95% CI: 1.93×10^5, 2.43×10^5]; U = 202, $p = 0.002$), Grade 2 (mean, 2.21×10^5 [95% CI: 2.03×10^5, 2.38×10^5]; U = 407, $p = 0.002$), and Grade 3 (mean, 2.16×10^5 [95% CI: 1.83×10^5, 2.49×10^5]; U = 46, $p = 0.01$). Similarly, CHII-rotational acceleration differed by CSP grade ($H(4) = 19.19$, $p < 0.001$); players with Grade 4 CSP had the highest CHII-rotational acceleration (mean, 2.36×10^7 [95% CI: 2.08×10^7, 2.64×10^7]), which was significantly greater than in Grades 0 (mean, 1.72×10^7 [95% CI: 1.56×10^7, 1.89×10^7]; U = 186, $p < 0.001$), 1 (mean, 1.78×10^7 [95% CI: 1.53×10^7, 2.02×10^7]; U = 200, $p = 0.0012$), and 2 (mean, 1.71×10^7 [95% CI: 1.56×10^7, 1.86×10^7]; U = 341, $p < 0.001$). Collectively, these findings indicate that more severe CSP grades, specifically Grade 4, are characterized by higher cumulative linear and rotational head impact exposure, whereas exposure frequency does not differ by CSP severity (Fig. 3 and Table 2).

Discussion

This study developed a revised CSP grading scale tailored for individuals with substantial exposure to RHI, including former contact- and collision-sport athletes. By incorporating posterior variants and more precisely delineating the extent of septal leaflet disruption, the revised scale addresses limitations of existing CSP classification systems and provides a more anatomically informative framework for clinical and research use in RHI populations. Applied to former American football players and unexposed asymptomatic controls, the revised scale demonstrated excellent inter-rater reliability. Former American football players also had significantly greater odds of being classified into a higher CSP grade than unexposed asymptomatic controls after adjustment for age, MRI acquisition site, APOE ε4 carrier status, eTIV, BMI, and years of education. Among former football players, 78.2% exhibited some degree of CSP. CSP length and volume

Table 2 | CSP Metrics

CSP Grade, n (%)	CSP Length, mm, mean (95% CI)	CSP Volume, mean (95% CI)	CHII-Frequency, mean (95% CI)	CHII-Linear Acceleration, mean (95% CI)	CHII-Rotational Acceleration, mean (95% CI)
Grade 0 37(21.8%)	0.27 [0.14, 0.40]	0.00 [0.00, 0.00]	1.08×10^4 [9.32×10^3, 1.22×10^4]	2.2×10^5 [1.97×10^5, 2.42×10^5]	1.72×10^7 [1.56×10^7, 1.89×10^7]
Grade 1 36(21.2%)	2.88 [2.36, 3.39]	7.98×10^{-6} [6.42×10^{-6}, 9.55×10^{-6}]	1.1×10^4 [9.29×10^3, 1.27×10^4]	2.18×10^5 [1.93×10^5, 2.43×10^5]	1.78×10^7 [1.53×10^7, 2.02×10^7]
Grade 2 65(38.2%)	5.45 [4.83, 6.06]	3.36×10^{-5} [2.72×10^{-5}, 4.00×10^{-5}]	1.03×10^4 [9.29×10^3, 1.14×10^4]	2.21×10^5 [2.03×10^5, 2.38×10^5]	1.71×10^7 [1.56×10^7, 1.86×10^7]
Grade 3 9(5.3%)	15.28 [10.05, 20.50]	1.61×10^{-4} [8.51×10^{-5}, 2.37×10^{-4}]	1.12×10^4 [6.74×10^3, 1.58×10^4]	2.16×10^5 [1.83×10^5, 2.49×10^5]	1.95×10^7 [1.67×10^7, 2.23×10^7]
Grade 4 23(13.5%)	—	—	1.22×10^4 [9.79×10^3, 1.46×10^4]	2.83×10^5 [2.5×10^5, 3.16×10^5]	2.36×10^7 [2.08×10^7, 2.64×10^7]

CSP morphology and cumulative head impact exposure in former American football players. Distribution of CSP grades among 170 former American football players. Grade 0 includes both the absence of CSP and a minimal cavum visible on only a single coronal slice; these participants were assigned a CSP volume of zero for statistical analyses. CSP length, normalized volume, and CHII measures are reported as means with corresponding 95% confidence intervals. CSP length and volume were not quantified for Grade 4 because septal leaflet discontinuity precluded reliable boundary delineation.

increased systematically across grades. Importantly, because the revised grading system was defined using anatomical landmarks rather than quantitative measurements, the increase in CSP length and volume across Grades 0–3 provides independent quantitative support for the construct validity of the classification scheme. In addition, players classified in the most severe CSP category (Grade 4) exhibited significantly greater cumulative linear and rotational head impact exposure than those classified as Grade 0, suggesting that more severe septal disruption may reflect greater lifetime biomechanical loading. Collectively, these findings establish the revised grading system as a reproducible, anatomically informed framework for characterizing CSP morphology and provide a standardized approach for investigating its relationship with cumulative RHI exposure.

The observed associations between CSP severity and cumulative head impact exposure provide insight into the potential biomechanical underpinnings of septal disruption in RHI-exposed individuals. The septal leaflets are particularly susceptible to shearing forces because of their midline location and tethering between the corpus callosum and the fornix[25,28]. Repeated mechanical loading may therefore produce progressive stretching, separation, and ultimately disruption of the septal leaflets, resulting in increasingly complex CSP morphology[7,18]. Consistent with this hypothesis, CSP length and volume increased progressively across grades, while the association between CSP severity and cumulative head impact exposure was driven primarily by participants classified as Grade 4. Because Grade 4 is defined by loss of septal leaflet integrity rather than posterior extension alone, it represents a qualitatively distinct morphological pattern that may reflect greater cumulative biomechanical loading. Although CSP has long been reported in autopsy-confirmed CTE and fenestrations of the septum pellucidum have been described at postmortem examination, these structural abnormalities are not specific to CTE and remain difficult to fully visualize using conventional 3 T MRI[1,31,36–41]. Importantly, CSP is also a common anatomical variant in healthy individuals[10,26,33,42–44], with reported prevalence varying substantially depending on imaging methodology, anatomical definition, and spatial resolution. This variability underscores that the mere presence of CSP is not specific to RHI[13] or CTE[37] and reinforces the importance of distinguishing subtle anatomical variants from the more severe morphological abnormalities captured by the revised grading system[24]. Accordingly, CSP should not be interpreted as an in vivo marker of CTE-associated tau pathology[37]. Rather, in the context of RHI, more severe CSP morphology may represent a structural imaging feature associated with cumulative biomechanical loading[7,12,13,16,18,25]. These findings support our previous work showing morphometric changes in former American football players with extensive RHI exposure[4–7,45–49]. Larger longitudinal studies will be necessary to determine whether Grade 4 represents progression along a continuum of septal disruption or a distinct anatomical phenotype[7,13,18,25].

More broadly, the present study highlights the importance of anatomically informed phenotyping when characterizing structural consequences of RHI. Existing CSP grading systems were developed for general clinical populations and rely primarily on qualitative or width-based assessments that incompletely capture the spectrum of septal morphologies observed in individuals with extensive RHI exposure[4,12,43,45]. By incorporating posterior extension, *cavum vergae* variants, and septal leaflet disruption into a single anatomically defined framework, the revised grading system provides greater phenotypic resolution while maintaining excellent reproducibility. Importantly, although quantitative measures of CSP length and volume were not used to assign grades, both increased systematically across the anatomically defined categories, providing independent quantitative validation of the classification scheme. While the present grading system was developed in former American football players, future studies should evaluate its applicability across other contact and collision sports, as well as in longitudinal cohorts spanning different stages of RHI exposure. Beyond the biological associations reported here, the principal contribution of this study is the development of a standardized, anatomically informed grading system for characterizing CSP morphology across MRI studies of RHI-exposed populations. Such a standardized anatomical framework may facilitate harmonization across research cohorts and imaging studies,

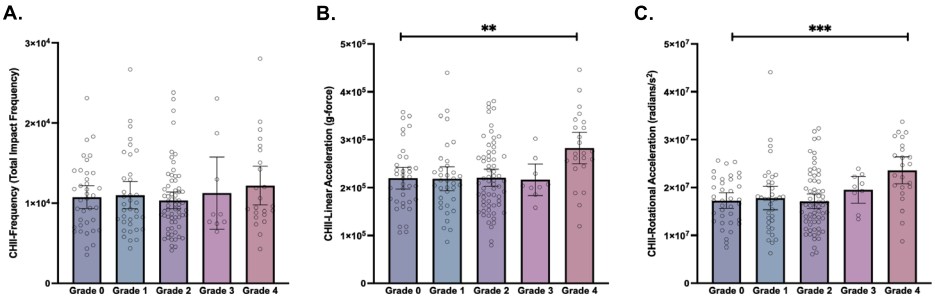

Fig. 3 | CSP Grade associations with head-impact exposure metrics. A CHII-frequency demonstrates no significant variation across CSP grades. **B** CHII-linear acceleration shows significant differences across grades $n = 170$, p = 0.007). **C** CHII-rotational acceleration likewise differs significantly across grades ($n = 170$, $p = 0.0007$). ** $p < 0.01$; *** $p < 0.001$. Error bars indicate 95% confidence intervals around the mean. A Kruskal-Wallis test followed by a Mann-Whitney U test was conducted for (**A**–**C**). All tests were two-sided, and adjustments were made for multiple comparisons. Abbreviation: CHII = Cumulative Head Impact Index.

improving the consistency and comparability of future investigations into the structural effects of RHI.

Overall, our revised CSP grading system provides a reproducible, anatomically informed framework for characterizing septal morphology in individuals with RHI exposure. This approach may facilitate future studies investigating relationships between CSP morphology, cumulative biomechanical exposure, and complementary neuroimaging, fluid, and clinical measures. Although the present findings support the biological relevance of CSP morphology in RHI-exposed individuals, they should not be interpreted as establishing CSP as an in vivo biomarker of CTE[50], as this study did not include neuropathological confirmation, longitudinal follow-up, or clinical outcome measures. Future longitudinal and multimodal studies integrating advanced neuroimaging, fluid biomarkers, and neuropathological validation will be necessary to determine the clinical significance of CSP morphology and its role within the broader spectrum of RHI-related neuroanatomical change.

This study has some limitations. First, the cohort consisted exclusively of male participants, limiting the applicability of the findings to females exposed to RHI. Second, because the sample included only former American football players, the generalizability of these results to athletes in other sports, such as soccer, ice hockey, or rugby, where the mechanical forces and patterns of head impact differ, remains uncertain. Third, cumulative RHI exposure was estimated using the CHII, which is derived from historical position- and level-specific head impact data rather than participant-specific biomechanical measurements. Although CHII is among the most widely used retrospective measures of cumulative RHI exposure, it cannot capture participant-specific variability in lifetime head impact exposure. Future studies incorporating participant-specific biomechanical measurements will be important for refining exposure estimates and evaluating their relationship with CSP morphology. Fourth, the cross-sectional design precludes conclusions about temporal changes in CSP morphology. Longitudinal studies are needed to determine whether CSP characteristics evolve and to distinguish RHI-related changes from those associated with typical aging. Fifth, participants in this cohort played American football between 1952 and 2007, a period marked by substantial changes in rules, style of play, and protective equipment, which may have influenced their cumulative head impact exposure. Finally, participants were recruited through advertisements, NFL alumni organizations, and targeted media outreach. As with many volunteer-based observational cohorts, this recruitment strategy may preferentially enroll individuals with greater concern regarding their neurological health, which could limit the generalizability of the findings to the broader population of former contact-sport athletes.

Conclusion

This study presents a revised, anatomically informed CSP grading scale that demonstrates excellent reliability and expected associations with cumulative head impact exposure among former American football players. By capturing structural variability that aligns with biomechanical mechanisms of septal disruption, the scale provides a more precise and reproducible framework for assessing CSP morphology in RHI-exposed individuals. As a standardized and anatomically informed framework, the revised grading system may facilitate harmonization across research cohorts and improve the consistency and comparability of future MRI studies investigating the structural consequences of RHI.

Data availability

Data from the DIAGNOSE CTE Research Project will be available to eligible investigators through the National Institutes of Health (NIH) Center for Information Technology. Interested investigators may also access DIAGNOSE CTE data, including the dataset used in this study, through a project-specific data-sharing portal. The raw dataset could not be made publicly available because detailed exposure information may permit identification of individual elite athletes. Questions about the data reported here can be directed to Dr. Hector Arciniega at Hector.Arciniega@nyulangone.org. Source data for Fig. 2 are provided in Supplementary Data 1.

Received: 14 April 2026; Accepted: 5 October 2026;
Published online: 24 October 2026

References

1. McKee A. C., et al. Neuropathologic and clinical findings in young contact sport athletes exposed to repetitive head impacts. *JAMA Neurol.* **80**, 1037–1050 (2023).
2. Nowinski, C. J. et al. Applying the Bradford Hill criteria for causation to repetitive head impacts and chronic traumatic encephalopathy. *Front. Neurol.* **13**, 938163 (2022).
3. Alosco, M. L. et al. Late contributions of repetitive head impacts and TBI to depression symptoms and cognition. *Neurology* **95**, e793–e804 (2020).
4. Jung, L. B. et al. Sulcal morphology in former American football players. *Brain Commun.* **7**, fcaf345 (2025).
5. John, O. et al. Shape analysis of the amygdala, hippocampus, and thalamus in former American football players. *Brain Commun.* **7**, 440 (2025).
6. Arciniega H., et al. Brain morphometry in former American football players: findings from the DIAGNOSE CTE research project. *Brain* **147**, 3596–3610 (2024).
7. Arciniega, H. et al. Cavum septum pellucidum in former American football players: findings from the DIAGNOSE CTE Research Project. *Neurol. Clin. Pract.* **15**, e200414 (2024).
8. Schwidde, J. T. Incidence of cavum septi pellucidi and cavum Vergae in 1032 human brains. *AMA Arch. Neurol. Psychiatry* **67**, 625–632 (1952).
9. Rakic, P. & Yakovlev, P. I. Development of the corpus callosum and cavum septi in man. *J. Comp. Neurol.* **132**, 45–72 (1968).
10. Sarwar, M. The septum pellucidum: normal and abnormal. *AJNR Am. J. Neuroradiol.* **10**, 989–1005 (1989).
11. Tubbs, R. S. et al. Cavum velum interpositum, cavum septum pellucidum, and cavum vergae: a review. *Childs Nerv. Syst.* **27**, 1927–1930 (2011).

12. Gardner, R. C. et al. Cavum Septum Pellucidum in Retired American Pro-Football Players. *J. Neurotrauma* **33**, 157–161 (2016).
13. Koerte, I. K. et al. Cavum Septi Pellucidi in Symptomatic Former Professional Football Players. *J. neurotrauma* **33**, 346–353 (2016).
14. Aviv, R. I., Tomlinson, G., Kendall, B., Thakkar, C. & Valentine, A. Cavum Septi Pellucidi in Boxers. *Can. Assoc. Radiol. J.* **61**, 29–32 (2010).
15. Kamps, S. et al. Cavum Septum Pellucidum (CSP) as a neuroimaging signature of head impact exposure compared to non-exposed patients with neurodegenerative disease and controls. *Alzheimer's. Dement.* **20**, e091209 (2024).
16. Stanwell, P. et al. Examining for cavum septum pellucidum and ventricular enlargement in retired elite-level rugby league players. *Front. Neurol.* **13**, 817709 (2022).
17. McAllister, D. et al. Neuroradiologic evaluation of MRI in high-contact sports. *Front. Neurol.* **12**, 701948 (2021).
18. Lee, J. K. et al. Association of Cavum Septum pellucidum and cavum vergae with cognition, mood, and brain volumes in professional fighters. *JAMA Neurol.* **77**, 35–42 (2020).
19. Lee, J. K. et al. Prevalence of traumatic findings on routine MRI in a large cohort of professional fighters. *AJNR Am. J. Neuroradiol.* **38**, 1303–1310 (2017).
20. Khanra, S., Srivastava, N. K., Chail, V. & Khess, C. R. Prevalence and characteristics of Cavum Septum pellucidum in schizophrenia: a 16 slice computed tomography study. *Indian J. Psychol. Med.* **38**, 455–459 (2016).
21. Degreef, G. et al. Increased prevalence of the cavum septum pellucidum in magnetic resonance scans and post-mortem brains of schizophrenic patients. *Psychiatry Res. Neuroimaging* **45**, 1–13 (1992).
22. Degreef, G., Lantos, G., Bogerts, B., Ashtari, M. & Lieberman, J. Abnormalities of the septum pellucidum on MR scans in first-episode schizophrenic patients. *AJNR Am. J. Neuroradiol.* **13**, 835–840 (1992).
23. Kwon, J. S. et al. MRI study of cavum septi pellucidi in schizophrenia, affective disorder, and schizotypal personality disorder. *Am. J. Psychiatry* **155**, 509–515 (1998).
24. Asken, B. M. et al. Linking type and extent of head trauma to cavum septum pellucidum in older adults with and without alzheimer disease and related dementias. *Neurology* **102**, e209183 (2024).
25. Kamps, S. et al. Enlarged cavum septum pellucidum as a neuroimaging signature of head impact exposure. *Brain Commun.* **7**, fcaf085 (2025).
26. Born, C. M. et al. The septum pellucidum and its variants. *Eur. Arch. Psychiatry Clin. Neurosci.* **254**, 295–302 (2004).
27. Siala, S., Homen, D., Smith, B. & Guimaraes, C. Imaging of the septum pellucidum: normal, variants and pathology. *Br. J. Radio.* **96**, 20221058 (2023).
28. Griffiths, P. D., Batty, R., Reeves, M. J. & Connolly, D. J. A. Imaging the corpus callosum, septum pellucidum and fornix in children: normal anatomy and variations of normality. *Neuroradiology* **51**, 337–345 (2009).
29. Shaw, C.-M. & Alvord, E. C. Jr Cava Septi Pellucidi Et Verg Æ: Their Normal And Pathological States1. *Brain* **92**, 213–224 (1969).
30. Agarwal, S., Chowdhury, K. & Chowdhury, L. D. Atypical presentation of Cavum Vergae. *Surg. Neurol. Int.* **16**, 378 (2025).
31. McKee, A. C. et al. Chronic traumatic encephalopathy (CTE): criteria for neuropathological diagnosis and relationship to repetitive head impacts. *Acta Neuropathol.* **145**, 371–394 (2023).
32. Alosco, M. L. et al. Developing methods to detect and diagnose chronic traumatic encephalopathy during life: rationale, design, and methodology for the DIAGNOSE CTE Research Project. *Alzheimers Res Ther.* **13**, 136 (2021).
33. Rios A., et al. High-resolution segmentation of the cavum septum pellucidum in young adult human brains. *Front. Neuroanat.* **19**, 1566762 (2025).
34. Fedorov, A. et al. 3D Slicer as an image computing platform for the quantitative imaging network. *Magn. Reson Imaging* **30**, 1323–1341 (2012).
35. Daneshvar, D. H. et al. Leveraging football accelerometer data to quantify associations between repetitive head impacts and chronic traumatic encephalopathy in males. *Nat. Commun.* **14**, 3470 (2023).
36. Bieniek, K. F. et al. The Second NINDS/NIBIB consensus meeting to define neuropathological criteria for the diagnosis of chronic traumatic encephalopathy. *J. Neuropathol. Exp. Neurol.* **80**, 210–219 (2021).
37. Alosco, M. L. et al. Structural MRI profiles and tau correlates of atrophy in autopsy-confirmed CTE. *Alzheimer's. Res. Ther.* **13**, 193 (2021).
38. McKee, A. C., Alosco, M. L. & Huber, B. R. Repetitive head impacts and chronic traumatic encephalopathy. *Neurosurg. Clin. North Am.* **27**, 529–535 (2016).
39. McKee, A. C., Stein, T. D., Kiernan, P. T. & Alvarez, V. E. The neuropathology of chronic traumatic encephalopathy. *Brain Pathol.* **25**, 350–364 (2015).
40. McKee, A. C. et al. The spectrum of disease in chronic traumatic encephalopathy. *Brain* **136**, 43–64 (2013).
41. Willis, M. D. & Robertson, N. P. Chronic traumatic encephalopathy: identifying those at risk and understanding pathogenesis. *J. Neurol.* **264**, 1298–1300 (2017).
42. Nopoulos, P. et al. Cavum septi pellucidi in normals and patients with schizophrenia as detected by magnetic resonance imaging. *Biol. Psychiatry* **41**, 1102–1108 (1997).
43. Wang, L.-X. et al. The Prevalence of Cavum Septum pellucidum in mental disorders revealed by MRI: a meta-analysis. *J. Neuropsychiatry Clin. Neurosci.* **32**, 175–184 (2019).
44. Trzesniak, C. et al. Are cavum septum pellucidum abnormalities more common in schizophrenia spectrum disorders? A systematic review and meta-analysis. *Schizophrenia Res.* **125**, 1–12 (2011).
45. Arciniega, H. et al. Dose-dependent white matter changes associated with repetitive head impacts in former American football players. *Brain Commun.* **8**, fcag195 (2026).
46. Wiegand, T. L. T. et al. Diffusion alterations at the gray matter/white matter boundary in traumatic encephalopathy syndrome. *J. Neurotrauma* **43**, 08977151251393966 (2025).
47. Jung, L. B. et al. Repetitive head impacts and perivascular space volume in former American football players. *JAMA Netw. Open* **7**, e2428687–e2428687 (2024).
48. Silk, T. et al. Cavum septum pellucidum in pediatric traumatic brain injury. *Psychiatry Res. Neuroimaging* **213**, 186–192 (2013).
49. Takahashi, T. et al. Prevalence of large cavum septi pellucidi and its relation to the medial temporal lobe structures in schizophrenia spectrum. *Prog. Neuropsychopharmacol. Biol. Psychiatry* **31**, 1235–1241 (2007).
50. Bernick, C. et al. Advancing biomarker development for chronic traumatic encephalopathy: Summary and recommendations from the 2025 Leon Thal Summit. *Alzheimers Dement* **22**, e71424 (2026).

Acknowledgements

We thank all study participants of the DIAGNOSE CTE Research Project for contributing to this research.

Author contributions

A.S.M., J.S., and B.S. contributed to drafting and revising the manuscript, study concept and design, and analysis and interpretation of data. M.E. contributed to the methods and data collection. R.D.F., S.B., D.H.D., C.H.A., C.B., L.J.B., J.L.C., E.M.R., R.A.S., and M.E.S. contributed to revising the manuscript for intellectual content and analysis and interpretation of data. R.J.R. and H.A. oversaw data acquisition, shaped the study design, contributed to interpretation of the findings, and made intellectual contributions to manuscript revision. DIAGNOSE CTE Research Project study team details are listed in Supplementary Table 4.

Funding
This study was supported by the National Institute of Neurological Disorders and Stroke U01NS093334 (JLC, EMR, MES, RAS), R21 NS140565 (HA); Alzheimer's Association Grant-25AARG-NTF-1377286 (HA), National Institute on Minority Health and Health Disparities Loan Repayment Program L32 MD016519 (HA), and Burroughs Wellcome Fund Postdoctoral Diversity Enrichment Program G-1022362.01 (HA).

Competing Interests
All authors declare no competing interests.

Additional information
Supplementary information The online version contains supplementary material available at https://doi.org/10.1038/s43856-026-01978-9.

Correspondence and requests for materials should be addressed to Hector Arciniega.

Peer review information *Communications Medicine* thanks all reviewer(s) for their contribution to the peer review of this work.

Reprints and permissions information is available at http://www.nature.com/reprints

Publisher's note Springer Nature remains neutral with regard to jurisdictional claims in published maps and institutional affiliations.

Open Access This article is licensed under a Creative Commons Attribution-NonCommercial-NoDerivatives 4.0 International License, which permits any non-commercial use, sharing, distribution and reproduction in any medium or format, as long as you give appropriate credit to the original author(s) and the source, provide a link to the Creative Commons licence, and indicate if you modified the licensed material. You do not have permission under this licence to share adapted material derived from this article or parts of it. The images or other third party material in this article are included in the article's Creative Commons licence, unless indicated otherwise in a credit line to the material. If material is not included in the article's Creative Commons licence and your intended use is not permitted by statutory regulation or exceeds the permitted use, you will need to obtain permission directly from the copyright holder. To view a copy of this licence, visit http://creativecommons.org/licenses/by-nc-nd/4.0/.

© The Author(s) 2026

This Article in Press is shared early to give you faster access to new research. It is citable and carries a permanent DOI. The final edited version will replace it automatically.

[1]Department of Rehabilitation Medicine, NYU Grossman School of Medicine, New York, NY, USA. [2]NYU Langone Concussion Center, NYU Langone Health, New York, NY, USA. [3]Brain Injury Research Center, Icahn School of Medicine at Mount Sinai, New York, NY, USA. [4]Department of Software Engineering and Information Technology, École de technologie supérieure, Université du Québec, Montréal, QC, Canada. [5]Department of Physical Medicine and Rehabilitation, Harvard Medical School, Boston, MA, USA. [6]Department of Physical Medicine and Rehabilitation, Massachusetts General Hospital, Boston, MA, USA. [7]Department of Physical Medicine and Rehabilitation, Spaulding Rehabilitation Hospital, Boston, MA, USA. [8]Department of Neurology, Mayo Clinic College of Medicine, Mayo Clinic Arizona, Scottsdale, AZ, USA. [9]Cleveland Clinic Lou Ruvo Center for Brain Health, Las Vegas, NV, USA. [10]Department of Neurology, University of Washington, Seattle, WA, USA. [11]Department of Neurology, NYU Grossman School of Medicine, New York, NY, USA. [12]Department of Population Health, NYU Grossman School of Medicine, New York, NY, USA. [13]Department of Ophthalmology, NYU Grossman School of Medicine, New York, NY, USA. [14]Chambers-Grundy Center for Transformative Neuroscience, Department of Brain Health, Kirk Kerkorian School of Medicine, University of Nevada, Las Vegas, Las Vegas, NV, USA. [15]Banner Alzheimer's Institute and Arizona Alzheimer's Consortium, Phoenix, AZ, USA. [16]Department of Psychiatry, University of Arizona, Phoenix, AZ, USA. [17]Department of Psychiatry, Arizona State University, Phoenix, AZ, USA. [18]Neurogenomics Division, Translational Genomics Research Institute and Alzheimer's Consortium, Phoenix, AZ, USA. [19]Department of Neurology, Boston University Alzheimer's Disease Research Center and CTE Center, Boston, MA, USA. [20]Department of Anatomy and Neurobiology, Boston University Chobanian & Avedisian School of Medicine, Boston, MA, USA. [21]Department of Neurosurgery, Boston University Chobanian & Avedisian School of Medicine, Boston, MA, USA. [22]Psychiatry Neuroimaging Laboratory, Department of Psychiatry, Brigham and Women's Hospital, Harvard Medical School, Boston, MA, USA. [23]Department of Radiology, Brigham and Women's Hospital, founding member of Mass General Brigham, and Harvard Medical School, Boston, MA, USA. [24]Department of Psychiatry, Massachusetts General Hospital, Boston, founding member of Mass General Brigham, Boston, MA, USA. [25]Institute for Translational Neuroscience, NYU Grossman School of Medicine, New York, NY, USA. [40]These authors contributed equally: Anya S. Mirmajlesi, Jared Stearns, Brian Szekely, Richard J. Rushmore, Hector Arciniega. *A list of authors and their affiliations appears at the end of the paper. ✉e-mail: hector.arciniega@nyulangone.org

for the DIAGNOSE CTE Research Project

Yi Su[26], Kewei Chen[26], Hillary Protas[26], Conni Boker[26], Rhoda Au[27], Robert C. Cantu[27], Lindsay Farrer[27], Robert Helm[27], Neil Kowall[27], Gustavo Mercier[27], James Otis[27], Jason Weller[27], Irene Simkin[27], Alondra Andino[28], Shannon Conneely[28], Courtney Diamond[28], Olivia Haller[28], Tennyson Hung[28], Nicole Gullotti[28], Megan Mariani[28], Brian Mayville[28], Kathleen McLaughlin[28], Mary Nanna[28], Taylor Platt[28], Sury Pulukuri[28], Fiona Rica[28], Madison Sestak[28], Michael McClean[29], Douglas Annis[29], Christine Chaisson[29], Carolyn Finney[29], Kerrin Gallagher[29], Kaitlin Hartlage[29], Jun Lu[29], Brett Martin[29], Emmanuel Ojo[29], Joseph N. Palmisano[29], Brittany Pine[29], Janani Ramachandran[29], Jennifer Fitzsimmons[30], Elena M. Bonke[30], Katherine Breedlove[30], Eduardo Coello[30], Hujiun Liao[30], Elizabeth Rizzoni[30], Vivian Schultz[30], Annelise Silva[30], Brynn Vessey[30], Sarah Banks[9], Jason Miller[9], Aaron Ritter[9], Marwan Sabbagh[9], Raelynn de la Cruz[9], Jan Durant[9], Morgan Golceker[9], Nicolette Harmon[9], Kaeson Kaylegian[9], Rachelle Long[9], Priscilla Sandoval[9], Robert W. Turner III[31], Kenneth L. Marek[32], Andrew Serrano[32], David W. Dodick[33], Yonas Geda[33], Jennifer V. Wethe[33], Bryce Falk[33], Amy Duffy[33], Marci Howard[33], Michelle Montague[33], Thomas Osgood[33], Debra Babcock[34], William Barr[35], Judith Goldberg[35], Thomas Wisniewski[35], Ivian Kirov[35], Yvonne Lui[35], Charles Marmar[35], Lisene Hasanaj[35], Liliana Serrano[35], Alhassan Al-Kharafi[35], Sammie Martin[35], Edward Riley[35],

William Runge[35], Elaine R. Peskind[36], Elizabeth Colasurdo[36], Daniel S. Marcus[37], Jenny Gurney[37], Keith A. Johnson[38] & Richard Greenwald[39]

[26]Banner Alzheimer's Institute, Phoenix, AZ, USA. [27]Boston University Chobanian & Avedisian School of Medicine, Boston, MA, USA. [28]Boston University, Boston, MA, USA. [29]Boston University School of Public Health, Boston, MA, USA. [30]Brigham and Women's Hospital, Boston, MA, USA. [31]George Washington University School of Medicine and Health Sciences, Washington, DC, USA. [32]Invicro, Needham, MA, USA. [33]Mayo Clinic Arizona, Phoenix, AZ, USA. [34]National Institute of Neurological Disorders and Stroke (NINDS), Bethesda, MD, USA. [35]New York University, New York, NY, USA. [36]University of Washington and VA Puget Sound, Seattle, WA, USA. [37]Washington University (CDNA), St. Louis, MO, USA. [38]Massachusetts General Hospital, Boston, MA, USA. [39]Simbex, Lebanon, PA, USA.